University of Utah
UNDERGRADUATE RESEARCH JOURNAL

CONVENTIONAL CT VERSUS WEIGHTBEARING CT IMAGING TECHNIQUES: A CADAVERIC EVALUATION

Katee Nicol Perez[1,2] (Faculty Mentor: Amy L. Lenz, PhD[2])
[1]Department of Biomedical Engineering, [2]Department of Orthopaedics

Abstract*— *Objective: **Biplane fluoroscopy has enabled model-based tracking of bones to capture in vivo bone kinematics. Model-based tracking requires digitally reconstructed radiographs (DRRs) to be created from patient-specific 3D bone models. Historically, models have been generated by segmenting bony anatomy from conventional CT images. Weightbearing CT (WBCT) scans can reduce the radiation dosage exposed to study participants without sacrificing high-resolution image quality. In addition, WBCT scans allow for kinematics from biplane fluoroscopy to be paired with robust 3D analyses to improve our understanding of the etiology of biomechanical pathologies. However, there is a lack of technical evaluations between conventional CT and WBCT imaging techniques to instill confidence that WBCTs can replace conventional CT imaging for accurately tracking data. We hypothesize that model-based tracking results from WBCT derived DRRs will be as effective as conventional CT derived DRRs. We aim to investigate WBCT compared to conventional-use clinical CT scanners with regards to accurate anatomical alignment, high-resolution images, low radiation dosage, and patient comfort and convenience. In this study a cadaver specimen (full foot and lower extremity) was used with both scanners. We found that bone reconstructions from WBCT scans were comparable to conventional CT images, and when used for model-based tracking they produced minor changes in kinematic results: less than 1.0 mm for translation and 1.0 degree rotation on average. Reliability between tracked solutions yielded excellent agreement further supporting the ability to use WBCT as a substitute for conventional CT images for model-based tracking for foot and ankle kinematics.**

***Index Terms*—Weight-bearing computerized tomography, conventional CT, biplane fluoroscopy, imaging, foot, ankle.**

This paper was submitted for review on February 28, 2022. This work was supported in part by the LS Peery Discovery Program Scholar Grant under #32712. *K. Perez is with the Department of Biomedical Engineering and the Department of Orthopaedics both located at the University of Utah, UT, USA.*
(Correspondence e-mail: katee.perez@utah.edu).

I. INTRODUCTION

ANKLE pain is experienced by 1 in every 5 young adults [1]. With a younger age range included, the number of ankle replacement surgeries worldwide has increased significantly over the past decade [2]. Ankle replacement surgeries are usually in response to serious ankle injuries and degenerative diseases, specifically osteoarthritis (OA) [2]. Ankle surgeries are invasive and in preparation for a successful procedure high resolution and reliable imaging techniques are required.

Traditionally, the conventional-use computerized tomography (CT) scanner has been the standard imaging modality for all major joint kinematic research. However, with the ankle joint, it is difficult to implement this standardized CT scanner [3-5]. The reason for such difficulty is, unlike other major joint anatomies, such as shoulder, hip, and knee; the ankle is a complex structure comprised of 6 different bones [6].

The most important ankle joint features are the subtalar and tibiotalar joint, as they are responsible for the wide range of movement of a healthy ankle

(Figure 1) [6]. Due to the substantial amount of overlapping surface area and depth of location, the subtalar and tibiotalar joints are often the first sites of OA development [7]. Therefore, there exists some limitations to obtaining high resolution images with using the conventional CT for image analysis of the subtalar and tibiotalar ankle joints [8, 9].

A collection of published articles has theorized that the implementation of a different imaging technique, the weight-bearing CT (WBCT) scanner, will overcome those limitations of the conventional CT [10-14]. The WBCT is said to have clear advantages over the conventional CT, including; (1) diagnostic reliability for kinematic data [12], (2) radiation dosage [13], (3) research and clinical institution cost [12, 14], and accurate alignment in static images [10]. Specifically in foot and ankle research, the use of WBCT has grown in popularity over the past 5 years [15]. Many important findings have relied on use of WBCT, including hindfoot alignment methods, or studies regarding subtalar and tibiotalar orientation and how it causes onset of osteoarthritis[16, 17]. However, such findings are limited to static measurements and 2D imaging. There is a lack of technical evaluations comparing conventional CT and WBCT use for accurately tracking biplane fluoroscopy data, which enables model-based tracking of *in vivo* bone kinematics [18]. A customized biplane fluoroscopy system for foot and ankle research is implemented to capture moving x-ray data and thus, expound upon static measurements with dynamic measurements of gait functionality. Replacing conventional CT with WBCT will influence all downstream design elements used with fluoroscopic imaging, thus altering the experimental methods. For every captured frame, digitally reconstructed radiographs (DRRs) created from patient-specific 3D bone models are aligned to the fluoroscopic captured data. Patient specific DRRs and 3Dmodels are sourced directly from segmenting CT images[19-21].

This paper aims to prove WBCT outperforms the use of conventional CT scanners through comparison of model-based tracking solutions from both CT modalities. We hypothesize WBCT will increase kinematic data accuracy of the subtalar and tibiotalar joints, along with the benefit of having accurate anatomical alignment, high-resolution images, low radiation dosage, and improved patient comfort and convenience. Model-based tracking solution analysis will determine the best image modality to be used to create 3D models in conjunction with fluoroscopic images from the biplane system [9, 10]. To mimic patient-data collections, this validation study features cadaveric specimen operations to accomplish WBCT and conventional CT model comparisons. To facilitate efficiency of workflow and eliminate human error with the above adjustments, a streamlined standard of work procedure (SOP) for biplane fluoroscopy calibration, segmentation from CT scans, and process for kinematic analysis through model-based tracking has been developed[22, 23]. A study proving WBCT is comparable to conventional CT has yet to be published and thus serves as the foundation of future patient data collections for foot and ankle research aimed at treating ankle degenerative diseases.

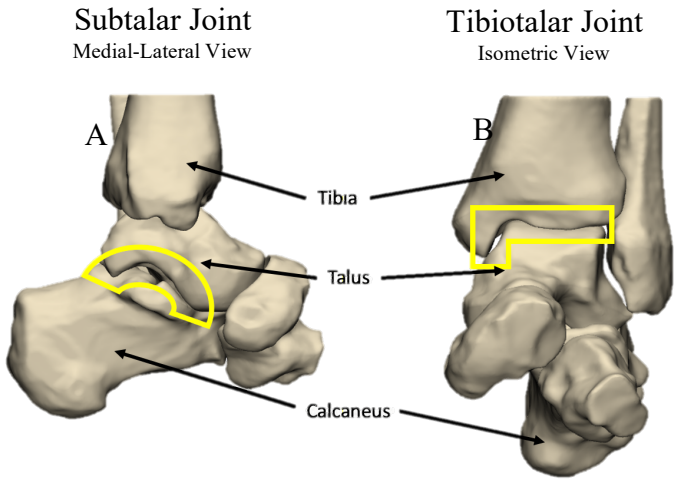

Figure 1: ***Ankle Anatomy*** *– (A) Subtalar joint seen from medial-lateral view. (B) Tibiotalar Joint seen from Isometric View. Joints indicated by yellow outlines. Arrows indicate location of Tibia, Talus, and Calcaneus; these three bones are featured in the results section below.*

II. BACKGROUND

Ankle replacement surgeries are increasing each year as the procedure and implant advancements improve. Important to note, the age range of ankle

surgery candidates has broadened to patients of younger ages for a similar reason [2]. In addition to skillful efforts in the operation room, there are many components which are necessary for a successful surgery; testing and development of implantation devices, diagnostic imaging of patients, and thorough analysis of patient kinematics. Each critical component can be improved upon in efficiency and precision with a highly accurate CT imaging technique. The conventional use CT does not allow the submillimeter and subvoxel precision needed to analyze the smaller structural units that make up the foot and ankle anatomy. Therefore, treatments of all kinds are limited by the current imaging standard with the conventional CT.

Clear imaging is significant in the work of orthopedic surgeries. As beforementioned, OA tends to develop within regions of the subtalar joint and tibiotalar joint for most patients [2, 3]. To properly treat these patients, it is important for researchers and surgeons alike to understand the patient-specific joint spacing of these regions, as it reveals gait functionality and bone spur morphology. Bone spurs or osteophyte can cause deformities abnormal to heathy joint space which allows for the many degrees of freedom in ankle movement [24]. The main difference seen between conventional CT and WBCT is the anatomical alignment of the patient's foot while imaged. Imaging while in weight-bearing stance appropriately reveals foot and ankle deformities. Several examples include diagnosing Varus and Valgus heel wedge alignment (tendency of heel to lean medially/laterally), arch collapse in the foot (introduces midfoot functionality), and cartilage deterioration to the structure as a whole. [8]. All these deformities are considered when identifying candidates for ankle surgeries such as total ankle replacement (TAR). Post-operative TAR kinematics are also tested to identify causation of such deformities [5].

A more in depth classification of WBCT exists in the publication with reference to the following factors; (1) diagnostic reliability, (2) availability, (3) patient-related cost, convenience and comfort, (4) radiation dosage, (5) research/ clinical cost [10-13]. This paper focuses on categories 1, 4 and 5 revealing conventional CT limitations while highlighting WBCT benefits. WBCT utilizes conical x-ray beam technology which circulates the subject limb within a minute. Fast turn-around time eliminates radiation exposure concern. Total radiation for both feet is averaged around 6 μSv (micro-Sieverts) for both feet, which is no more than the average X-ray [9]. Cone-beam based WBCT technology has been seen since 1996, primarily in the dental industry [9]. Therefore, its emergence is not recent, and availability is secure. Specific to the orthopaedic research laboratory, the WBCT in house is yet to be operable for clinical use. Further investigation provided by this and other papers along with proper funding will readily enable the WBCT for clinical use for incoming patients [6, 10-14] .

Bringing attention to cone-beam based WBCT in a validation study could potentially enable specialized procedures for foot and ankle analysis, and later knee and pelvic [9]. One procedure specialized for foot and ankle research, is the implementation of a customized biplane fluoroscopy. As stated before, clinical biplane fluoroscopy systems were previously utilized amongst all orthopaedic research regardless of anatomy differences. Improvements to *in vivo* methods of orthopaedic kinematics has been frequent over the past several years, specifically, publications focused on model-based tracking [19, 23]. Model-based tracking is an advanced non-invasive method of quantifying joint movement, and it has proven to increase accuracy of results in comparison to prior methods. Prior methods such as skin-based motion capture tracking and single plane markerless tracking. Skin-based motion tracking failed to capture movement of the deeply embedded tibiotalar and subtalar joints[25]. Other model-based methods in the past utilized a single plane approach, thus hindering proper alignment [6]. Publications over the past decade have led to biplane fluoroscopy; a non-invasive, dual-plane, in vivo method to quantify bone kinematics [19, 23]. Today, this system is the standardized method for most orthopaedic research [6-9, 19, 23, 26]. Validation of off-the-shelf clinical biplane fluoroscopy, in conjunction with conventional CT, for kinematic applications is well established for shoulder, pelvic, knee and ankle studies [5, 9]. However, these major joint structures

have distinct characteristics and cannot all be held to an identical standardized quantification method. Creation of a customized, dual plane or biplane fluoroscopy system is an additional step towards improving foot and ankle research. Fluoroscopic image capture is much like a continuous moving X-Ray at an adjusted speed. During fluoroscopic trials, the patient subject is asked to perform certain actions such as normal gait, or double heel rise. These motions are captured over roughly 300+ frames and later processed to obtain kinematic data of the patient's motion. Biplane fluoroscopy methodology relies heavily on the use of digitally reconstructed radiographs (DRRs). The theoretical process of creating DRR's is well established; once a bone model is generated, bone density data from the CT scan is rendered into a 2D model [26]. With pre-established components, part of this study's objective was to determine a method of execution with a new biplane system, and two new software platforms. New components introduce different obstacles in how to obtain and process data. Calculations to maintain global coordinate systems and spatial dimensions have been manipulated and checked, transitioning from raw files to segmentation software, then dynamic tracking requires transition between several or more software platforms. Implemented software includes, but is not limited to Materialise Mimics and 3-Matic, C-Motion Dynamic Stereo X-Ray, ImageJ, Phantom Camera Control Application, CORVIEW, MeshLab, etc.

Biplane fluoroscopy can also be used as a diagnostic tool in clinical settings. However, fluoroscopic images are primarily used in research to investigate the function of a post-operative TAR limb [5, 26]. The components of a biplane fluoroscopy system consist of two X-Ray emitters and two image intensifiers arranged orthogonally to provide dual plane set of images. To enable X-ray capture of the foot and ankle, this set up is placed nearly on ground level. Other components may include a force place and a walkway to provide additional measurements on a patient's gait ability (Figure 2). Fluoroscopic images are the parameters upon which model-based tracking of bone models and digitally reconstructed radiographs (DRR's) are aligned to collect kinematic data. Model-based

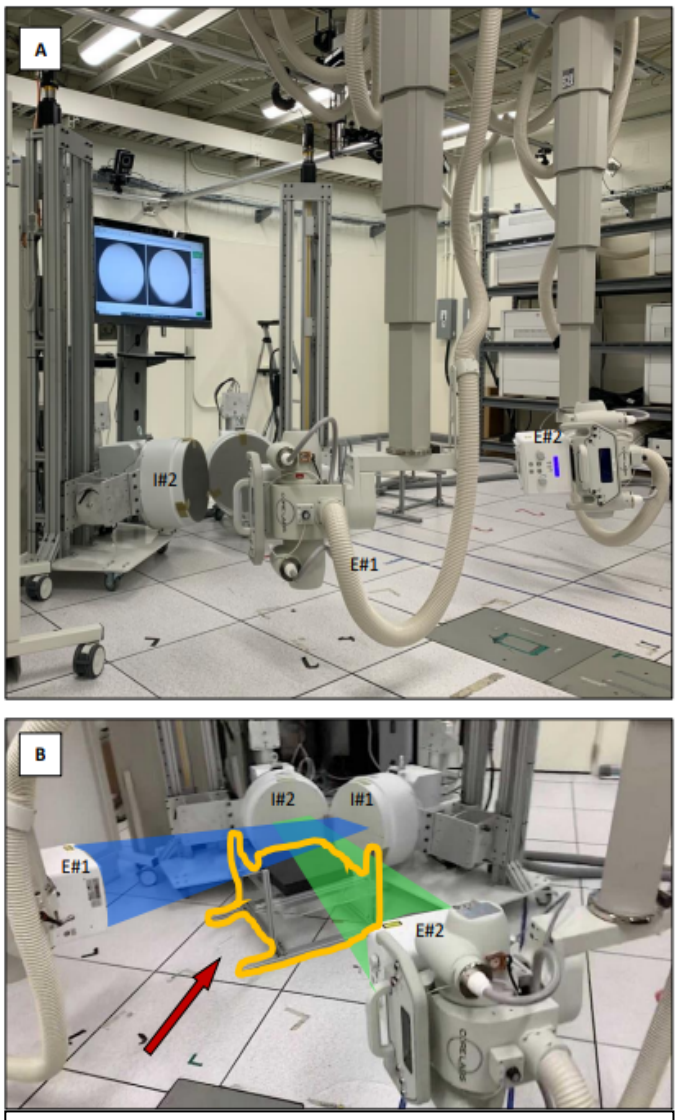

*Figure 2**: Biplane Fluoroscope** – (A) Emitters 1 and 2, and image intensifier 1 are labeled. Ceiling fixtures allow mobility of equipment and alignment downwards into the floor. (B) Force plate is mimicked with Styrofoam platform seated on an acrylic table in center of orthogonal arrangement of biplane fluoroscopy setup.*

tracking is the phase of the experimental methods where all components from CT scan segmentation and fluoroscopic image data, from the biplane system, come together.

Validation studies of biplane fluoroscopy systems feature a comparison of invasive and non-invasive measurement procedures of bony structures [5]. Comparisons are performed through model-based tracking; which is done for the purpose of validating

the biplane fluoroscopy sub-millimeter (mm) and sub-degree (deg) kinematic accuracy. Invasive measurement is accomplished by implanting radiopaque beads, 1.0 mm in diameter, into a cadaveric specimen's bone structures. The implanted beads serve as markers, not subject to displacement and easily identifiable in x-ray imaging. Non-invasive measurements rely on bone density distinction between trabecular and cortical surfaces; thus referred to as model-based tracking. For living bone, non-invasive methods are the only acceptable option. Thus, verification of biplane fluoroscopy is accomplished when bead-based and model-based tracking solutions prove to be identical and highly accurate. Use of "golden" standard beads holds relevance to the image modality comparison, as it will serve as an adjunct to further verify the upgraded biplane fluoroscopy system. The remainder of this paper will refer to the biplane fluoroscopy system as the customized dual-plane system specific to the foot and ankle research lab.

For all patient types, accuracy across imaging components must be ensured to properly diagnose and treat OA. Certain methodologies are well established, however imaging instrumentation has advanced and needs to be implemented into the streamlined workflow. A rigid workflow is needed for future researchers to follow and for data to be systematically processed and analyzed. Once validated, the WBCT scanner with biplane fluoroscopy will later be used for cerebral palsy patients, outside the scope of targeting those with common ankle deformities.

III. METHODS

In efforts to prove WBCT outperforms the conventional use of clinical CT scanners through comparison, this cadaveric validation study developed a new standards of procedure to take place of prior experimental methods. All steps in the new methods design are outlined in separate documentation known as the SOP for tracking. Our lab anticipates the interaction of a volunteered patient with the new biplane fluoroscopy system and to be imaged using the WBCT scanner. Prior to this, the new methods design must be tested.

A. Experimental Overview

To enable repeated testing, we utilized a frozen cadaver specimen; male, age 63, inclusive of entire foot, ankle and full length of Tibia and Fibula shaft. Sourcing for this and all cadaveric specimens are obtained through associated body donor programs of the University of Utah. This specimen was screened and showed no signs of osteoarthritis or previous damage to the anatomy before use in this study, thus it is classified as asymptomatic. First, two main data sets were obtained from the WBCT and conventional CT, and both captures were done prior to data collection for the biplane fluoroscopy system. Second, customized biplane fluoroscopy system parameters were troubleshooted to obtain clear fluoroscopic images to aid in tracking. Third, all data was brought into software processing to be segmented, calibrated and optimized for tracking. Troubleshooting errors while using these numerous applications have been recorded and addressed in the SOP, as an all-encompassing data process to include preparations for data collection, data collection and calibration, to post-analysis and results, to avoid issues of time consumption and tediousness. Collaboration with software developers about the above-listed platforms has been a crucial source of aid in analyzing kinematic data. Such collaborations have led to developer updated executables online to improve user accommodations. Finally, a model for each bone for both CT scanners were tracked against the same fluoroscopic data. This data collection promotes statistically relevant data supporting WBCT efficiency and precision for foot and ankle research. In addition, bone model reconstruction comparisons were made between segmented 3D models for all three bones segmented from both CT scanners.

B. Image Acquisition with Weight-bearing and Conventional-use CT

Use of Styrofoam and plastic molds helped to keep the cadaver stationary while capturing CT images. While using the WBCT, the cadaver was position upright within the instrument. For this reason the tibial shaft of the WBCT is distinctly

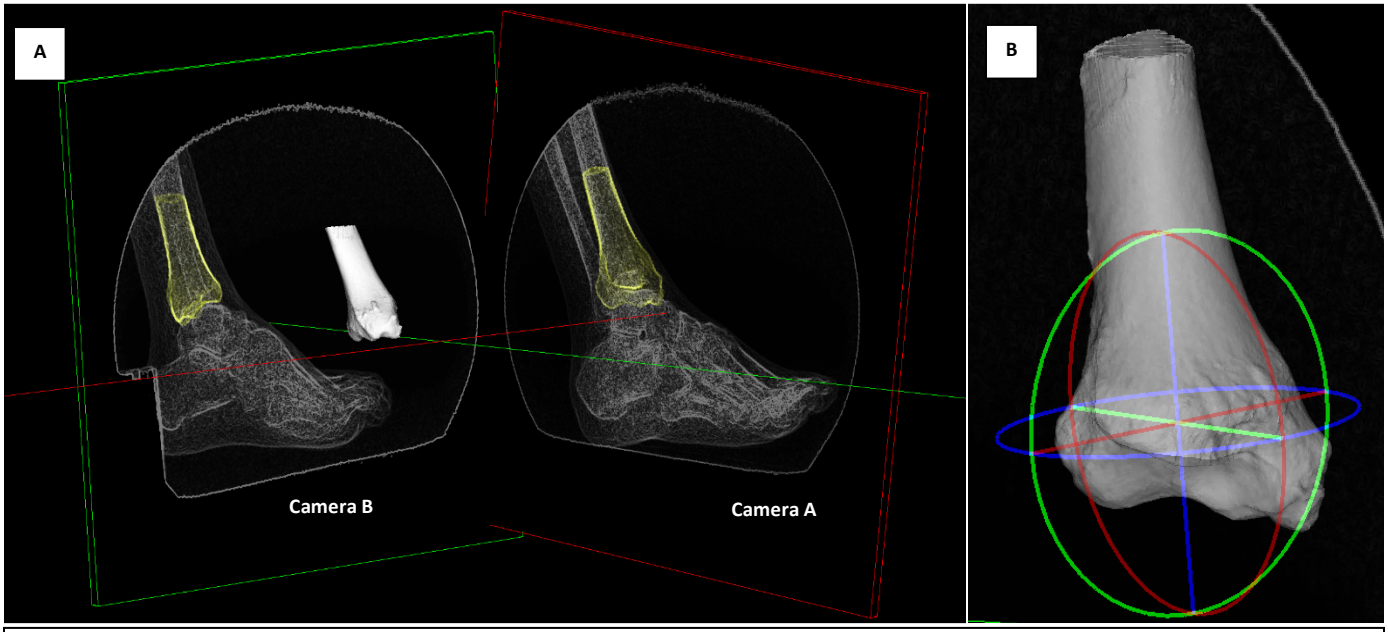

*Figure 3:**Biplane Fluoroscopy Setup for Model-Based Tracking** – (A) Model-based tracking aligns the Tibia DRR (yellow surface) to the radiographic images (black & white X-ray images). Image parameters are adjusted to increase definition of cortical bone morphology. DSX suite, X4D, enables manipulation of DRR and Tibia object (white surface) with six degrees of freedom: X-Y-Z translation and rotation. (B) Axis of rotation and translation appear when bone object is selected. Bone surface is from WBCT.*

shorter than that of the conventional use CT, which was position to lay across the table while being imaged. The following image parameters were established after four trials when using the biplane fluoroscopy system: 100 frames per second (fps), 60 kilovolts (kV), 50 milliampere (mA), 1000 exposure (exp), 500 effective dose rate (EDR). With these values, high-resolution images are obtained in both camera A and B images seen in the virtual lab (Figure 3). It was discovered these image parameters must be maintained across all data trials, referring to "whites", "grids", etc. for proper calibration.

C. Image Acquisition with Biplane Fluoroscopy System

For the purposes of the study, only the Tibia, Talus, and Calcaneus were evaluated. The cadaver leg is positioned to mimic a weight-bearing stance while in use of the WBCT. Anatomical planes of motion, such as gait function, are simulated manually when fluoroscopic data is captured within the limits of the emitters field of view (FOV) (Figure 2). Three parameters are needed for calibrating the biplane fluoroscopy system. First, "whites" establish contrast parameters for when field of view is void of any object. This is performed by capturing a small number of frames using the image intensifiers and X-ray emitters while there is no subject disrupting the orthogonal rays. Second, "grids" are performed to correct for distortion around the perimeter of the image intensifiers. This is accomplished by attaching stainless steel grid plates to the flat surfaces of each of the intensifiers. The spaces between the grid lines are captured and adjusted afterwards for correction. Lastly, we use a custom-built calibration cube with 64 beads placed specifically inside in known locations. This is done to establish the spatial orientation of the two image intensifiers with relation to each other to define the 3D space where the ankle subject is centered. These beads form a 4x4x4 lattice with 64 mm spacing between the beads (Figure 4). Lego pieces are known to be manufactured within 0.002 mm of accuracy, making the calibration cube to be highly precise[20]. In addition to these 64 beads, there are also 4 uniquely shaped tokens, each in their own specified location. These tokens are manually selected during the calibration process using one of the new software platforms, and from

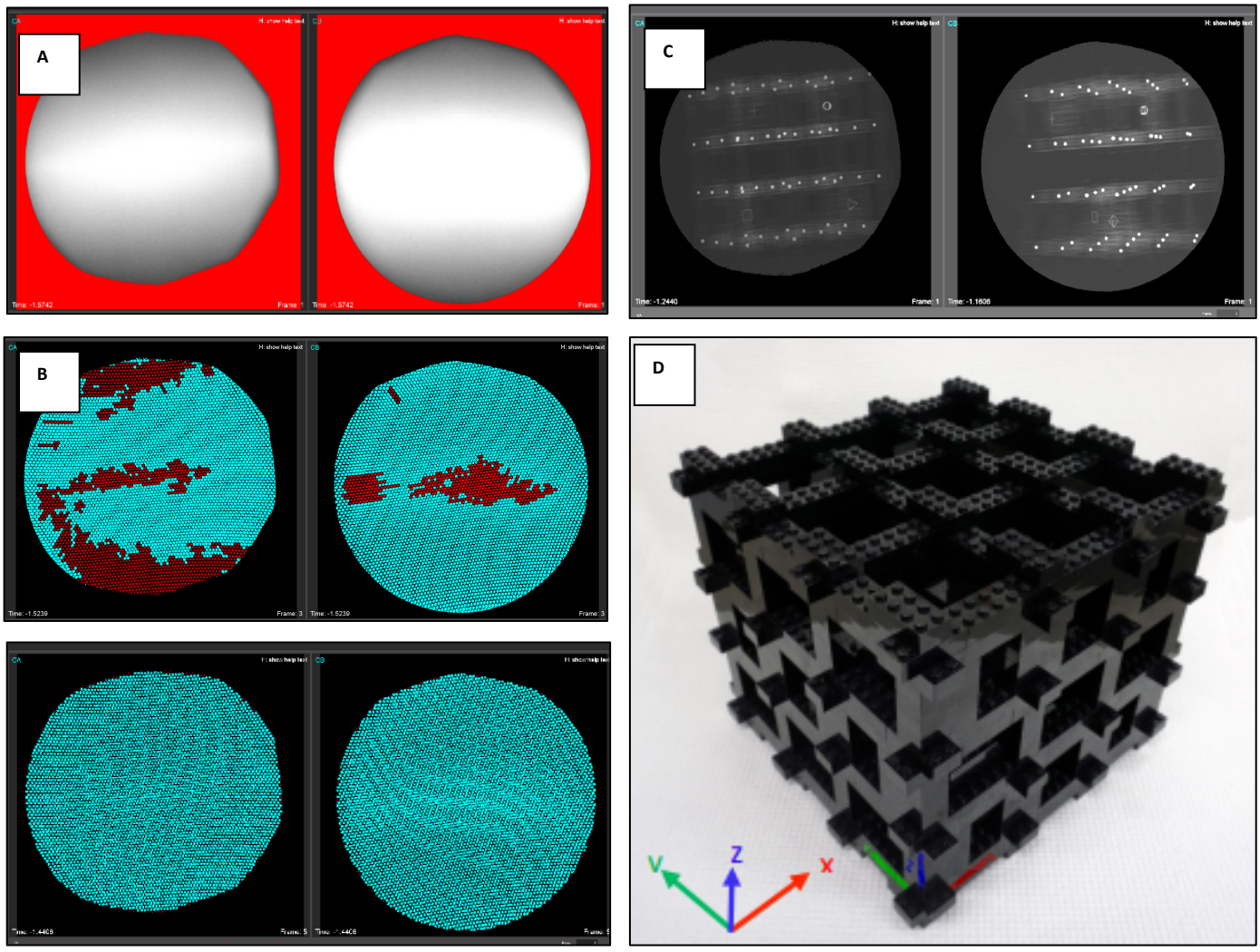

Figure 4: ***Calibration*** *– (A) "Whites" visualized within DSX. Shadows within FOV differ between camera A and camera B. Elimination of shadow by narrowing FOV proves best for image contrast. (B) "Grids" captured by the process described. Distortion is corrected by adjusting the pixel sizes of the spaces between the grid lines. Bottom image features the corrected FOV. Preliminary data featured camera A FOV smaller compared to camera B FOV. (C) Radiographic images of Lego calibration cube captures 4x4x4 lattice of 64 beads and 4 unique token shapes. Two angles of view are used for 3D spatial orientation of the space. (D) The calibration cube with beads and tokens located inside Lego pieces.*

identification of their arrangements the rest of the 64 beads can be automatically identified [20].

D. Post-processing Software for all Data Collections

Subscription to the following 3D motion capture data analyzing software enables the lab to perform calibrations: C-Motion: Dynamic Stereo X-ray (DSX v.1.05.6367) and Materialise: Mimics (v.24.0) and 3-matic (v.16.0) have enabled calibrations. DSX* provides control over the calibration parameters to ensure the best resolution and use of our fluoroscopic data. Once calibration is done properly, "Static" and "Dynamic" trials are synchronized to prepare for tracking. Static refers to a few hundred frames of the specimen whilst held still, dynamic trials are of the same length only moving functions are captured. These trials consist of radiographic images, or X-ray images of the ankle subject within the orthogonal field of view (FOV). Preliminary fluoroscopic captures consist of 600 frames of data, of which 60 select frames, manually tracked in intervals of 10 have been studied for this report. 60 frames displayed enough movement

within the dynamic trials with this data set. Manual tracking 10 frames apart was optimal for the auto-tracking software to work efficiently. These 60 frames will be referred to as test frames. The same radiograph images in camera A and camera B are maintained when using two different bone models to perform model-based tracking. This establishes frame time and image parameter consistency.

E. Segmentation from WBCT and Clinical CT

Materialize platforms; Mimics and 3-matics, offer tools for CT image stack segmentation from all three anatomical views. In addition to 3D digital models, segmentation allows for isolation of Hounsfield units (HU) to the attributing bone tissue. Unique DRRs are developed for each bone. These capture the bones' density and enables researchers to visualize the difference between cortical and trabecular bone. Optimization of DRR's against X-ray images to better visualize this contrast is performed in DSX, X4D. [27]. Cortical bone has higher density than trabecular bone, therefore, it is seen as a bright contour against the black and white X-ray images. For the bone model comparison, models are superimposed and part comparison calculations show differences in the morphology which indicate sub voxel clarity of the CT images.

F. Model-Based Tracking Methodology

Tracking is one of the final steps of validation and is utilized generally across research fields in orthopaedics. CT data of a bone is aligned frame-by-frame with time synchronized radiographic data. The positions or poses of the bone are recorded and saved as graphical solutions of the bone's local coordinate system[5]. The high-definition of cortical bone enables model-based tracking. Reconstructed bone models are rotated and translated along six degrees of freedom (DOF) within the global coordinate system, key-framing every 50 frames (Figure 3). This is repeated until a trackable range is covered. Once completed, a tool is used to spline pose maps together to calculate a good approximation for intermittent frames which were not tracked manually. Comparisons of these changes in millimeters and degrees are made between the model derived from WBCT and clinical CT. The results of this comparison over the range of the specified test frames are discussed in the following section.

G. Statistical Analysis

The kinematic results from models created from conventional CT and WBCT were then compared. All surface reconstructions and tracked solution differences are reported in mean, standard deviations (SD), median, 1st quartile, and 3rd quartile from paired T-test statistical analysis. Interclass correlations (ICCs) were calculated between tracked solutions for WBCT versus conventional CT. A study using WBCT scans to accurately track biplane fluoroscopy data has yet to be published, and thus serves as the foundation of future patient data collections to frontier foot and ankle research.

IV. RESULTS

The bone model reconstruction comparison found little to no changes between those created from conventional CT and WBCT scans. ICCs for all x, y, z translations and rotations were >0.9, indicating excellent agreement. The mean segmentation differences between WBCT and conventional CT for the tibia, talus, and calcaneus were 0.16, -0.14, and 0.18 mm respectively (Table 1). Each segmentation difference was within the resolution of conventional CT (0.6 mm) (Figure 6). All tracked kinematic differences between conventional CT and WBCT for the talus, calcaneus, and tibia were less than 1.0 mm for translation and 1.0-degree rotation on average (Figure 7, Table 2). The tracking software enabled a comma delimited file export for each pose map. Data analysis table generated in data analysis spreadsheet programs. Preliminary results from model-based tracking consist of ten tracked frames, each manually verified for accuracy and consistency between the two imaging modalities. Bias exists with regards to attention to anatomical differences and attention to alignment because of two different researchers each tracking one of the CT models. The tracking software enabled a comma delimited file export for each pose map.

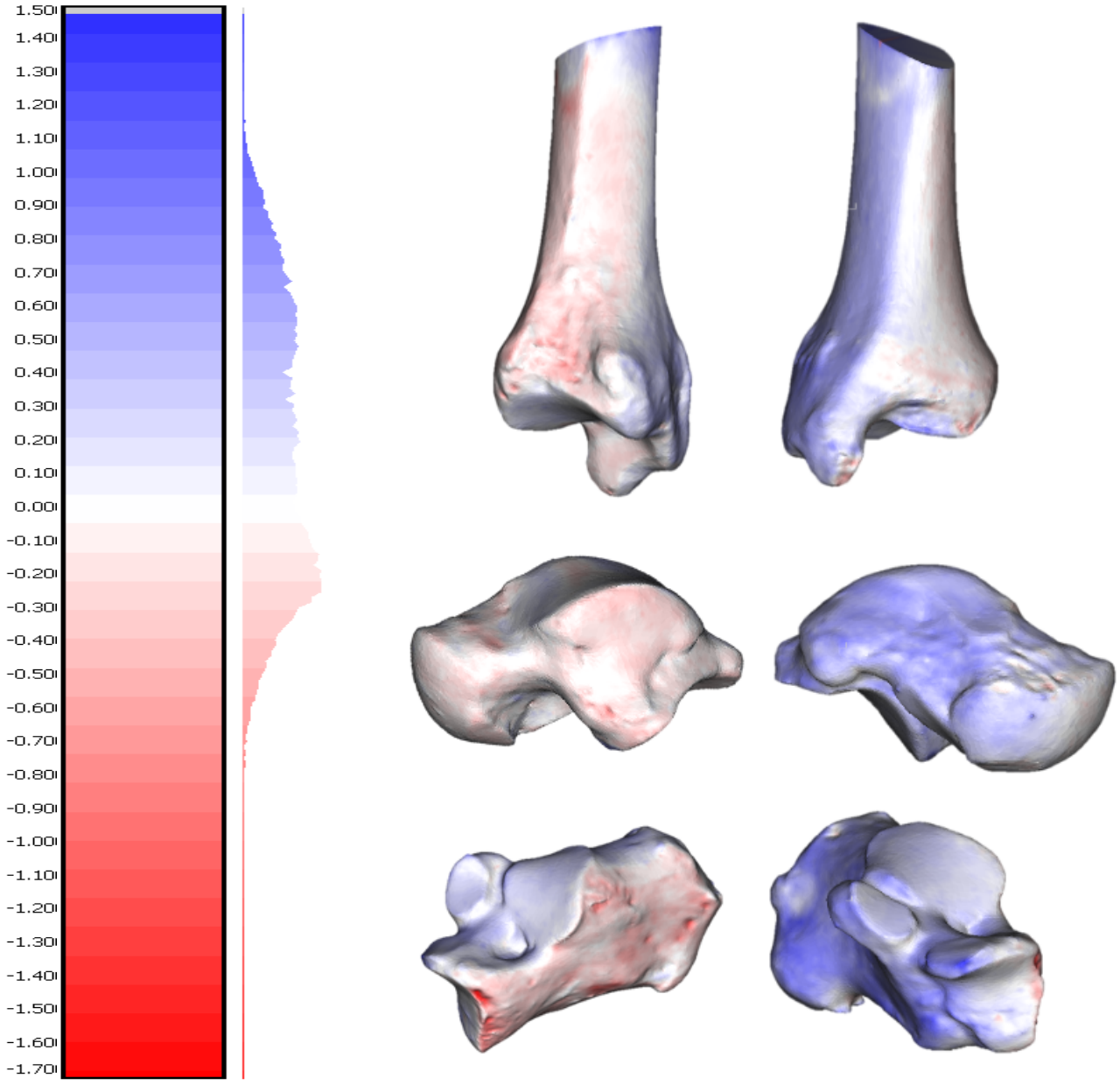

Figure 6: ***Segmentation Differences Colormap***– This color map shows the distances between the surfaces of the two models and projects the values of these distances onto the red, white and blue models to the right of the color map. This color map ranges from -1.7 mm to 1.5 mm. Red indicates regions of oversampling from the conventional CT, blue indicates regions of under-sampling from the conventional CT.

Table 1. 3D reconstruction differences between imaging modalities.

Segmentation Differences Between WBCT versus CT (mm)

	Mean	SD	Q1	Median	Q3
Tibia	0.16	-0.36	-0.15	0.14	0.49
Talus	-0.14	0.31	-0.37	-0.10	0.10
Calcaneus	0.18	0.51	-0.26	0.18	-0.65

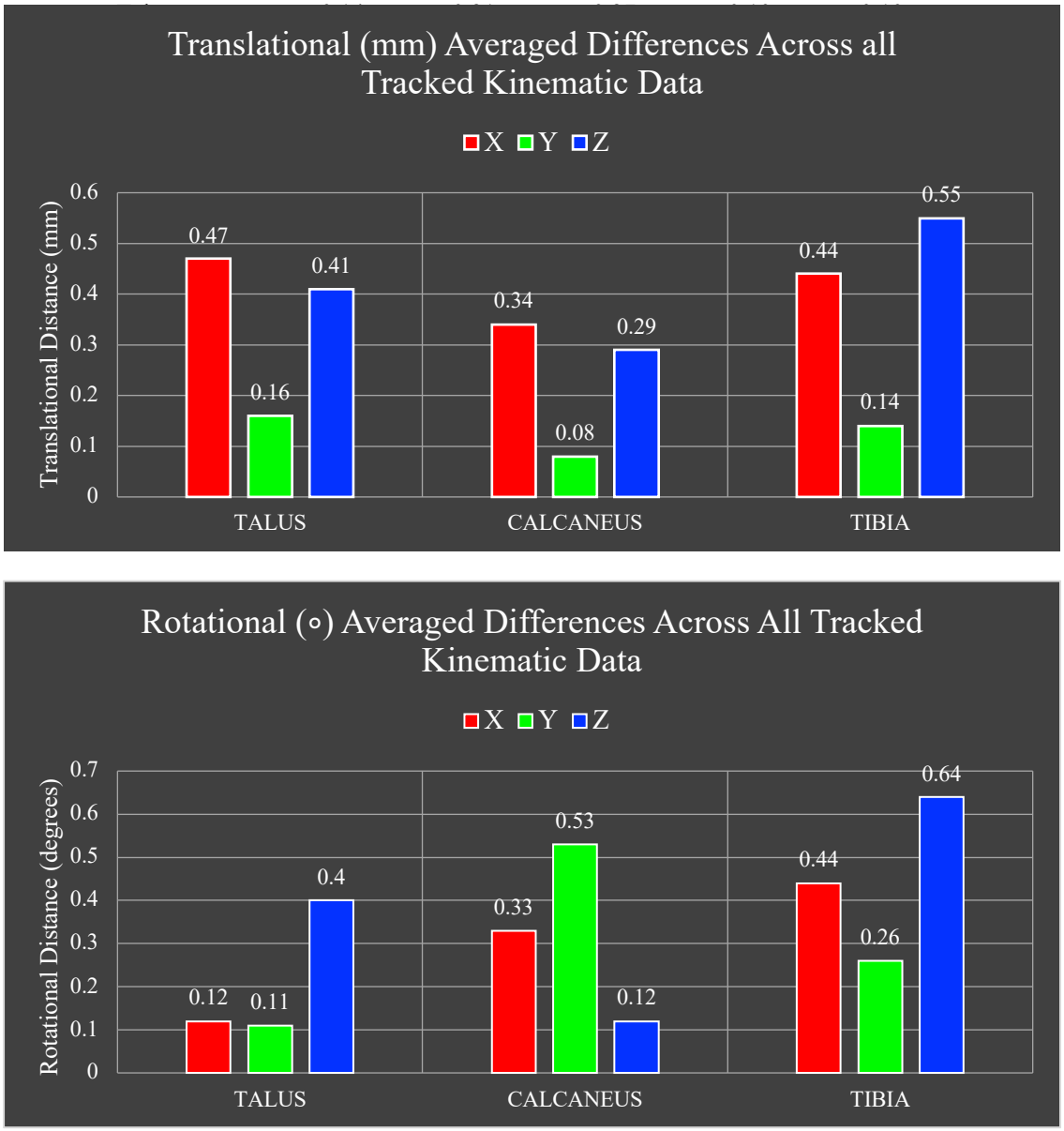

Figure 7: ***Kinematic Differences Histogram***–Differences between every solved pose for every frame of the tracked kinematic data were calculated, and the averages are graphed. ***Top Graph -*** the translational differences along the x, y and z axis for the Tibia, Talus, and Calcaneus. ***Bottom Graph -*** the rotational differences about the x, y and z axis for the same 3 bones. All averages across tracked data is less than 1 mm or 1 degree of difference.

Table 2. Kinematic differences between model-based tracking for WBCT versus conventional CT DRRs. All axes are noted and represent 6 degrees of freedom by which the models were aligned.

	Translation (mm)			Rotation (°)		
	X	Y	Z	X	Y	Z
Talus						
SD	0.36	0.11	0.32	0.15	0.14	0.47
Q1	0.52	0.2	0.33	0.02	0.04	0.18
Median	0.61	0.23	0.53	0.13	0.11	0.47
Q3	0.81	0.27	0.68	0.3	0.25	0.56
Calcaneus						
SD	0.08	0.04	0.09	0.18	0.27	0.09
Q1	0.27	0.05	0.23	0.2	0.36	0.05
Median	0.33	0.08	0.29	0.31	0.49	0.11
Q3	0.4	0.11	0.37	0.45	0.68	0.15
Tibia						
SD	0.26	0.08	0.29	0.32	0.18	0.38
Q1	0.27	0.08	0.33	0.17	0.11	0.35
Median	0.4	0.13	0.49	0.4	0.23	0.56
Q3	0.56	0.19	0.79	0.65	0.4	0.96

V. DISCUSSION

Weightbearing CT (WBCT) scans can image bony anatomy with higher resolution than conventional CT imaging techniques while reducing radiation exposure to study participants by using cone-beam technology [28]. The objective was to validate the high-resolution biplane fluoroscopy system using WBCT scans to compare to the established conventional CT scans. Conventional CT has been the standard for CT imaging, and to prove WBCT is close in agreement encourages confidence in models made from WBCT scans. Along with benefits in the clinical setting, the WBCT could also enable higher resolution images and improve model generating accuracy for research and diagnostic purposes. Validation using a cadaveric specimen enabled repeated use of WBCT and clinical CT scanners, as well as preliminary use of the customized biplane fluoroscopy system located. Segmentation from CT data was processed to construct 3D bone models and digitally reconstructed radiographs (DRRs). These elements are reconfigured to be used in model-based tracking. Tracking is critical in comparing the two imaging modalities, as it proves WBCT incorporated into fluoroscopy tracking outputs accurate kinematic data of gait functionality similar to the conventional CT. Results indicated that the bone reconstructions from WBCT scans were comparable to those created from conventional CT images, and that when used for model-based tracking they produced minor changes in kinematic results. Q1 describes the first quartile value, which is the threshold value for 25% of data points when arranged sequentially. Q3

Figure 8: ***Models of Both Image Modalities –*** *FOV of CT scanners result in differing Tibial and Fibular shaft lengths. An example of a Tibia bone derived from WBCT isolates the distal end from the rest of the tibial shaft, whereas the proximal end of the shaft is included entirely from the clinical CT.*

describes the third quartile value, which is the threshold value for 75% of the data points when arrange sequentially. These quartile values combined offer insight into the dispersion range of the model reconstruction differences and the kinematic differences (Tables 1 and 2). All averages comparing rotational differences are less than 1.0 degree and translational differences are less than 1.0 mm. This is a clear indication that using 3D models from the WBCT to be used in tracking to align to the fluoroscope images can be favored over the conventional CT. However, there is a larger difference seen in the z translation and rotation for all 3 bones. The z rotational differences could be due to the fact such changes are difficult to spot when viewing the biplane lab setup (Figure 3). These rotational changes move the bone models in or out of the plane, therefore, these are slightly expected results. However, most unexpected are the z translational differences being the largest, especially considering the Tibia bones. The tibia has the greatest advantage with bone morphology tracking due to its longer shaft in the z direction providing a large surface area to aid in the semiautomatic positioning of the bone. Observing that the tibia between the conventional CT and the WBCT produced the largest disagreement does not offer a direct cause of effect. Several factors are considered the cause of this observed disagreement in the z translation. Tracking bias is a factor. Tracking range could also be factor, considering it is centered along the progression of heel touch to toe-off. Often the center of this gait progression features to widest range of movement seen throughout the whole captured range. Another factor, which could be seen as a limitation of the study, is in regard to the WBCT cropping out the full Tibia shaft from view (Figure 8). This contrasts with the conventional CT which may even capture the distal femur depending on the height of the imaged patient. Secondary limitations of the study include the WBCT image parameter configuration. The WBCT image parameters were yet to be properly configured, thus resulting in our preliminary images to be poor in quality. Once WBCT configuration was completed through trial-and-error, the image results were clear enough to be processed through Materialise-Mimics for segmentation. Another limitation exists with only one researcher overlooking the semiautomatic model-based tracking for all 6 bone models (3 from conventional CT and 3 from WBCT). Due to the tedious nature of model-based tracking, multiple researchers are recommended to analyze tracked frames in a series of passes to eliminate human-error based inconsistencies. This leads into future work plans for this validation study. The tracking range is to be expanded and more researchers are to peer-review this dataset. In addition, bead implants to the cadaver will further prove WBCT matches conventional CT kinematic analysis. Beads indicate a “gold standard” for tracking, as they provide clear markers of the bone’s anatomy. This will overcome the limitation which exists with model-based tracking alone as it introduces segmentation errors and image quality differences between the two scanners. Confidence in replacing the conventional CT is due to the high level of agreement data of kinematic data, in addition to the lower cost, lower radiation dosage, and lower degree of inconvenience for patients [10-14].

VI. REFERENCES

[1] C. L. Hill, T. K. Gill, H. B. Menz, and A. W. Taylor, "Prevalence and correlates of foot pain in a population-based study: the North West Adelaide health study," (in eng), *J Foot Ankle Res,* vol. 1, no. 1, p. 2, Jul 28 2008, doi: 10.1186/1757-1146-1-2.

[2] T. A. Perry, A. Silman, D. Culliford, L. Gates, N. Arden, and C. Bowen, "Trends in the Utilization of Ankle Replacements: Data From Worldwide National Joint Registries," (in eng), *Foot Ankle Int,* vol. 42, no. 10, pp. 1319-1329, Oct 2021, doi: 10.1177/10711007211012947.

[3] M. Horisberger, V. Valderrabano, and B. Hintermann, "Posttraumatic ankle osteoarthritis after ankle-related fractures," (in eng), *J Orthop Trauma,* vol. 23, no. 1, pp. 60-7, Jan 2009, doi: 10.1097/BOT.0b013e31818915d9.

[4] N. Krahenbuhl, L. Zwicky, L. Bolliger, S. Schadelin, B. Hintermann, and M. Knupp, "Mid- to Long-term Results of Supramalleolar Osteotomy," *Foot Ankle Int,* vol. 38, no. 2, pp. 124-132, Feb 2017, doi: 10.1177/1071100716673416.

[5] R. Zaidi *et al.*, "The outcome of total ankle replacement: a systematic review and meta-analysis," (in eng), *Bone Joint J,* vol. 95-b, no. 11, pp. 1500-7, Nov 2013, doi: 10.1302/0301-620x.95b11.31633.

[6] J. A. Cross, B. D. McHenry, R. Molthen, E. Exten, T. G. Schmidt, and G. F. Harris, "Biplane fluoroscopy for hindfoot motion analysis during gait: A model-based evaluation," (in eng), *Med Eng Phys,* vol. 43, pp. 118-123, May 2017, doi: 10.1016/j.medengphy.2017.02.009.

[7] A. L. Lenz *et al.*, "Compensatory Motion of the Subtalar Joint Following Tibiotalar Arthrodesis: An in Vivo Dual-Fluoroscopy Imaging Study," *J Bone Joint Surg Am,* vol. 102, no. 7, pp. 600-608, Apr 1 2020, doi: 10.2106/JBJS.19.01132.

[8] L. Baverel, J. Brilhault, G. Odri, M. Boissard, and F. Lintz, "Influence of lower limb rotation on hindfoot alignment using a conventional two-dimensional radiographic technique," (in eng), *Foot Ankle Surg,* vol. 23, no. 1, pp. 44-49, Mar 2017, doi: 10.1016/j.fas.2016.02.003.

[9] J. D. Mozingo *et al.*, "Validation of imaging-based quantification of glenohumeral joint kinematics using an unmodified clinical biplane fluoroscopy system," *J Biomech,* vol. 71, pp. 306-312, Apr 11 2018, doi: 10.1016/j.jbiomech.2018.02.012.

[10] A. Barg *et al.*, "Weightbearing Computed Tomography of the Foot and Ankle: Emerging Technology Topical Review," *Foot Ankle Int,* vol. 39, no. 3, pp. 376-386, Mar 2018, doi: 10.1177/1071100717740330.

[11] A. Del Rio *et al.*, "Weightbearing Cone-Beam Computed Tomography of Acute Ankle Syndesmosis Injuries," (in eng), *J Foot Ankle Surg,* vol. 59, no. 2, pp. 258-263, Mar-Apr 2020, doi: 10.1053/j.jfas.2019.02.005.

[12] A. L. Godoy-Santos, A. Bernasconi, M. Bordalo-Rodrigues, F. Lintz, C. F. T. Lôbo, and C. C. Netto, "Weight-bearing cone-beam computed tomography in the foot and ankle specialty: where we are and where we are going - an update," (in eng), *Radiol Bras,* vol. 54, no. 3, pp. 177-184, May-Jun 2021, doi: 10.1590/0100-3984.2020.0048.

[13] F. Lintz, P. Beaudet, G. Richardi, and J. Brilhault, "Weight-bearing CT in foot and ankle pathology," (in eng), *Orthop Traumatol Surg Res,* vol. 107, no. 1s, p. 102772, Feb 2021, doi: 10.1016/j.otsr.2020.102772.

[14] J. A. Carrino *et al.*, "Dedicated cone-beam CT system for extremity imaging," (in eng), *Radiology,* vol. 270, no. 3, pp. 816-24, Mar 2014, doi: 10.1148/radiol.13130225.

[15] M. S. Conti and S. J. Ellis, "Weight-bearing CT Scans in Foot and Ankle Surgery," (in eng), *J Am Acad Orthop Surg,* vol. 28, no. 14, pp. e595-e603, Jul 15 2020, doi: 10.5435/jaaos-d-19-00700.

[16] J. Z. Zhang, F. Lintz, A. Bernasconi, and S. Zhang, "3D Biometrics for Hindfoot Alignment Using Weightbearing Computed Tomography," (in eng), *Foot Ankle Int,* vol. 40, no. 6, pp. 720-726, Jun 2019, doi: 10.1177/1071100719835492.

[17] N. Krähenbühl, L. Siegler, M. Deforth, L. Zwicky, B. Hintermann, and M. Knupp,

"Subtalar joint alignment in ankle osteoarthritis," (in eng), *Foot Ankle Surg,* vol. 25, no. 2, pp. 143-149, Apr 2019, doi: 10.1016/j.fas.2017.10.004.

[18] M. J. Bey, S. K. Kline, R. Zauel, T. R. Lock, and P. A. Kolowich, "Measuring dynamic in-vivo glenohumeral joint kinematics: technique and preliminary results," (in eng), *J Biomech,* vol. 41, no. 3, pp. 711-4, 2008, doi: 10.1016/j.jbiomech.2007.09.029.

[19] S. M. Geiger, E. Reich, P. Bottcher, S. Grund, and J. Hagen, "Validation of biplane high-speed fluoroscopy combined with two different noninvasive tracking methodologies for measuring in vivo distal limb kinematics of the horse," *Equine Vet J,* vol. 50, no. 2, pp. 261-269, Mar 2018, doi: 10.1111/evj.12717.

[20] B. J. Knörlein, D. B. Baier, S. M. Gatesy, J. D. Laurence-Chasen, and E. L. Brainerd, "Validation of XMALab software for marker-based XROMM," (in eng), *J Exp Biol,* vol. 219, no. Pt 23, pp. 3701-3711, Dec 1 2016, doi: 10.1242/jeb.145383.

[21] C. J. Tan, W. C. H. Parr, W. R. Walsh, M. Makara, and K. A. Johnson, "Influence of Scan Resolution, Thresholding, and Reconstruction Algorithm on Computed Tomography-Based Kinematic Measurements," (in eng), *J Biomech Eng,* vol. 139, no. 10, Oct 1 2017, doi: 10.1115/1.4037558.

[22] WIKIsysop. "X4D X-Ray and DRR Settings." https://c-motion.com/v3dwiki/index.php?title=X4D_X-ray_and_DRR_Settings (accessed.

[23] J. M. Iaquinto *et al.*, "Model-based tracking of the bones of the foot: A biplane fluoroscopy validation study," (in eng), *Comput Biol Med,* vol. 92, pp. 118-127, Jan 1 2018, doi: 10.1016/j.compbiomed.2017.11.006.

[24] Y. M. Golightly *et al.*, "Relationship of Joint Hypermobility with Ankle and Foot Radiographic Osteoarthritis and Symptoms in a Community-Based Cohort," (in eng), *Arthritis Care Res (Hoboken),* vol. 71, no. 4, pp. 538-544, Apr 2019, doi: 10.1002/acr.23686.

[25] J. A. Nichols, K. E. Roach, N. M. Fiorentino, and A. E. Anderson, "Subject-Specific Axes of Rotation Based on Talar Morphology Do Not Improve Predictions of Tibiotalar and Subtalar Joint Kinematics," *Ann Biomed Eng,* vol. 45, no. 9, pp. 2109-2121, Sep 2017, doi: 10.1007/s10439-017-1874-9.

[26] D. J. Blair, A. Barg, K. B. Foreman, A. E. Anderson, and A. L. Lenz, "Methodology for Measurement of in vivo Tibiotalar Kinematics After Total Ankle Replacement Using Dual Fluoroscopy," (in eng), *Front Bioeng Biotechnol,* vol. 8, p. 375, 2020, doi: 10.3389/fbioe.2020.00375.

[27] "X4D X-ray and DRR Settings." https://c-motion.com/v3dwiki/index.php?title=X4D_X-ray_and_DRR_Settings (accessed.

[28] M. Richter, B. Seidl, S. Zech, and S. Hahn, "PedCAT for 3D-imaging in standing position allows for more accurate bone position (angle) measurement than radiographs or CT," (in eng), *Foot Ankle Surg,* vol. 20, no. 3, pp. 201-7, Sep 2014, doi: 10.1016/j.fas.2014.04.004.